Mixed-Metal Cluster Chemistry. 13. Syntheses and Isomer Distribution Studies of $Cp_2W_2Ir_2(\mu\text{-}CO)_3(CO)_{7-n}(PR_3)_n$ (n = 1, 2; R = Ph, Me): X-ray Crystal Structure of $Cp_2W_2Ir_2(\mu\text{-}CO)_3(CO)_6(PPh_3)$

Susan M. Waterman and Mark G. Humphrey*

Department of Chemistry, Australian National University, Canberra, ACT 0200, Australia

Jeanne Lee

Department of Chemistry, University of New England, Armidale, NSW 2351, Australia

Graham E. Ball

NMR Facility and School of Chemistry, University of New South Wales, Sydney, NSW 2052, Australia

David C. R. Hockless

Research School of Chemistry, Australian National University, Canberra, ACT 0200, Australia

Received December 16, 1998

Reactions of $Cp_2W_2Ir_2(CO)_{10}$ (**1**) with n equivalents of PPh_3 and PMe_3 (n = 1, 2) proceed in dichloromethane at room temperature to afford the clusters $Cp_2W_2Ir_2(\mu\text{-}CO)_3(CO)_{7-n}(PPh_3)_n$ (n = 1 (**2**), 2 (**3**)) and $Cp_2W_2Ir_2(\mu\text{-}CO)_3(CO)_{7-n}(PMe_3)_n$ (n = 1 (**4**), 2 (**5**)), respectively, in reasonable yields (38−63%). These products exhibit ligand fluxionality in solution, resolvable at low temperature into the constituent interconverting isomers. A structural study of one isomer of **2**, namely **2a**, reveals that the three edges of a WIr_2 face of the tetrahedral core are spanned by bridging carbonyls and that the iridium-bound PPh_3 ligates axially and the tungsten-bound cyclopentadienyl ligands coordinate apically and axially with respect to the plane of bridging carbonyls. Information from this crystal structure and ^{13}C and ^{31}P NMR spectral data have been employed to assign coordination geometries for the isomers of **2**−**5**. NMR studies included development and use of 2D triple-resonance experiments with carbonyl cluster complexes; these $^1H-^{31}P-^{13}C$ correlation experiments, designed to elucidate P−C coupling networks involving phosphorus and carbonyl ligands (a "HPCO experiment"), benefit from the sensitivity enhancement gained from using proton detection. All the isomers of clusters **2**−**5** contain a carbonyl-bridged WIr_2 basal plane and an apical tungsten atom; ligands can be approximately coplanar (radial) to the basal plane or below the plane (axial). The configuration of **2a** (axial phosphine, axial Cp, apical Cp), as assigned by NMR spectroscopy, is consistent with the structural determination. A second configuration (**2b**, **4b**: axial phosphine, axial Cp, apical Cp) is the only one identified (within the temperature range 183−293 K) for the PMe_3-substituted cluster **4**. Two isomers, both with radial phosphine, axial phosphine, axial Cp, apical Cp configurations, have been identified for **5**, namely **5a** and **5b**; it is likely that isomers of **3** adopt the same configurations. The WIr_2-bridged form is seen exclusively across the isomers, indicating that the presence of two electropositive tungsten atoms may be polarizing the electron distribution toward the iridiums, although steric factors may also be involved.

Introduction

The ligand substitution chemistry of homometallic clusters, particularly $Ir_4(CO)_{12}$, has been studied extensively,[1] but ligand replacement at heterometallic clusters has been the subject of comparatively fewer reports. The studies of $Ir_4(CO)_{12}$ have been extended to $Ir_3Rh(CO)_{12}$ and $Ir_2Rh_2(CO)_{12}$,[2−5] with differences to the parent cluster ascribed to the differing electropositivities

* To whom correspondence should be addressed. Ph: (+61) 2 6249 2927. Fax: (+61) 2 6249 0760. E-mail: Mark.Humphrey@anu.edu.au.

(1) Abel, E. W., Stone, F. G. A., Wilkinson, G., Eds. *Comprehensive Organometallic Chemistry II*; Pergamon Press: Oxford, U.K., 1995.

(2) Bondietti, G.; Laurenczy, G.; Ros, R.; Roulet, R. *Helv. Chim. Acta* **1994**, *77*, 1869.

(3) Bondietti, G.; Ros, R.; Roulet, R.; Grepioni, F.; Braga, D. *J. Organomet. Chem.* **1994**, *464*, C45.

(4) Laurenczy, G.; Bondietti, G.; Merbach, A. E.; Moullet, B.; Roulet, R. *Helv. Chim. Acta* **1994**, *77*, 547.

(5) Bondietti, G.; Suardi, G.; Ros, R.; Roulet, R.; Grepioni, F.; Braga, D. *Helv. Chim. Acta* **1993**, *76*, 2913.

10.1021/om9810246 CCC: $18.00
Publication on Web 06/21/1999

of the metals. The tetrahedral mixed-metal clusters $CpWIr_3(CO)_{11}$ and $Cp_2W_2Ir_2(CO)_{10}$ (**1**) are conceptually derived from $Ir_4(CO)_{12}$ by successive replacement of $Ir(CO)_3$ vertexes with one or two $CpW(CO)_2$ units and, in comparison to the iridium−rhodium clusters, incorporate the significantly more electropositive metal tungsten. We have previously reported the synthesis and characterization of ligand-substituted derivatives of $CpWIr_3(CO)_{11}$, namely $CpWIr_3(\mu\text{-}CO)_3(CO)_{8-n}(L)_n$ (L = PPh_3, PMe_3; $n = 1-3$),[6] and have recently reported the isomer distribution at these clusters.[7] The electropositive tungsten did not appear to polarize the electron distribution toward the iridium atoms, as may have been expected; the WIr_2-bridged form was predominant across the isomers of $CpWIr_3(\mu\text{-}CO)_3(CO)_{8-n}(L)_n$, whereas an Ir_3 basal plane is expected if the electron distribution is polarized toward the iridium atoms. We now extend our studies to include the substitution reactions of $Cp_2W_2Ir_2(CO)_{10}$ (**1**), which contains two electropositive tungsten atoms, and report identification of the geometries of the clusters $Cp_2W_2Ir_2(\mu\text{-}CO)_3(CO)_{7-n}(L)_n$ (L = PPh_3, $n = 1$ (**2**), 2 (**3**); L = PMe_3, $n = 1$ (**4**), 2 (**5**)), and a comparison of isomer structure to the tungsten−triiridium and tetrairidium systems.

Experimental Section

General Information. All reactions were performed under an atmosphere of dry nitrogen (high-purity grade, BOC), although no special precautions were taken to exclude air during workup. The reaction solvents were dried and distilled under nitrogen using standard methods: CH_2Cl_2 over CaH_2 and thf from sodium/benzophenone. All other solvents were reagent grade and were used as received. Petroleum ether refers to a fraction of boiling point range 60−80 °C. The products of thin-layer chromatography were separated on 20 × 20 cm glass plates coated with Merck GF_{254} silica gel (0.5 mm). $Cp_2W_2Ir_2(CO)_{10}$ was prepared by the published procedure.[8] ^{13}CO-enriched samples were prepared from ^{13}CO-enriched (90%) **1**, itself obtained by stirring a solution of the cluster in CH_2Cl_2 under 1.2 atm of ^{13}CO at 25 °C for 48 h. Triphenylphosphine (Aldrich) and trimethylphosphine (Aldrich, 1 M solution in THF) were purchased commercially and used as received.

Physical Measurements. Infrared spectra were recorded on a Perkin-Elmer System 2000 Fourier transform spectrophotometer with NaCl optics. ^1H NMR spectra were recorded on a Varian Gemini 300 spectrometer (300.0 MHz). ^{13}C and ^{31}P NMR spectra were recorded on a Varian VXR300S spectrometer (^{13}C at 75.4 MHz and ^{31}P at 121.4 MHz) or a Bruker DMX500 (^{13}C at 125.7 MHz) and are proton-decoupled. $^1H-^{31}P-^{13}C$ triple-resonance experiments were recorded on a Bruker DMX500 (^1H at 500.1 MHz, ^{31}P at 202.5 MHz, ^{13}C at 125.7 MHz) or a Bruker DMX600 (^1H at 600.1 MHz, ^{31}P at 242.9 MHz, ^{13}C at 150.9 MHz). $^{183}W-^{13}C$ and $^{183}W-^1H$ correlation experiments were recorded on a Bruker DMX600 (^{183}W at 24.9 MHz, ^1H at 600.1 MHz, ^{13}C at 150.9 MHz). Spectra were run in $CDCl_3$ (Cambridge Isotope Laboratories), CD_2Cl_2 (Cambridge Isotope Laboratories), acetone-d_6 (Cambridge Isotope Laboratories), or $CDFCl_2$;[9] chemical shifts in ppm are referenced to internal residual solvent (^1H, $CHCl_3$ at 7.26 ppm; ^{13}C, CD_2Cl_2 at 53.8 ppm, acetone-d_6 at 29.8 ppm, and $CDCl_3$ at 77.0 ppm) or external 85% H_3PO_4 (^{31}P, H_3PO_4 at 0.0 ppm).

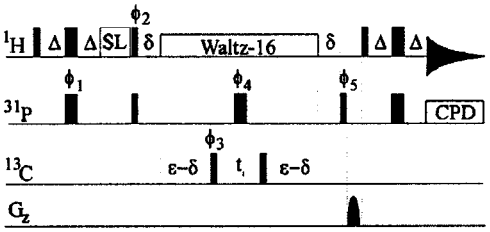

Figure 1. Pulse sequence used for triple-resonance HPCO experiment. Narrow bars represent 90° pulses and wide bars 180° pulses. SL denotes a spin lock pulse (1.5 ms). Typical delays used were $\Delta = 20.8$ ms ($\approx {}^1/_4 J_{PH}$), $\delta = 9.8$ ms, and $\epsilon = 38.5$ ms ($\approx {}^1/_2 J_{PC}$, optimized for ${}^nJ_{PC} = 13$ Hz in this case). Phase cycles used were $\phi_1 = x, -x$; $\phi_2 = y, -y$; $\phi_3 = 2x, 2(-x)$; $\phi_4 = 8x, 8y, 8(-x), 8(-y)$; $\phi_5 = 4x, 4(-x)$; Receiver = $x, -x, -x, x, -x, x, x, -x, -x, x, x, -x, x, -x, -x, x$. A minimum of 8 scans per increment was employed. Inclusion of the gradient pulse (1 ms, sine shaped, ca. 28 G cm^{-1}) is optional, and more gradients should be incorporated in cases where the ^{13}C is not labeled and suppression of unwanted signals is important. In a typical experiment at a temperature of 183 K, 256 FID were collected in t_1 of 1024 t_2 points each. Spectral widths were 2.24 ppm in F_2 (^1H), resulting in an acquisition time of 0.46 s and 92.0 ppm in F_1 (^{13}C). A recycle delay of 0.3 s was used. High-power 90° pulse widths were 9.4, 7.8, and 10.4 μs for ^1H, ^{31}P, and ^{13}C, respectively.

On the 500 and 600 MHz instruments, ^{31}P shifts were measured relative to hypothetical external 85% H_3PO_4 using $\Xi = 40.480\,737$ and ^{183}W shifts were measured relative to hypothetical external WF_6 (WF_6 at 0 ppm) using $\Xi = 4.161\,733$ using the formula X (nucleus reference frequency) = $\Xi \times$ (^1H zero ppm frequency)/100.[10] Small differences in ^{31}P shifts obtained on 300 and 500 MHz instruments are ascribed to the differences in referencing techniques used.

Resonances are reported in the following form: ppm (assignment; multiplicity; relative intensity). The specific assigned sites are shown in Figure 8. The ^1H NOESY experiments were carried out using the standard pulse sequence with the mixing time set to 0.2 s. The integrated ^{13}C NMR spectra were recorded with a recycle delay of 3−5 times the longest T_1 value of the carbonyl ligands. $^1H-^{31}P$ HSQC experiments were recorded using the standard sequence, including refocusing and decoupling. Typically, delays were optimized for a 12 Hz coupling to emphasize $^2J_{PH}$ correlations or 4 Hz to emphasize long-range correlations to the Cp protons. $^1H-^{31}P-^{13}C$ triple-resonance experiments were acquired using the pulse sequence shown in Figure 1. $^{31}P-^{13}C$ and $^{13}C-^{183}W$ correlations were recorded using a standard HMQC sequence with proton decoupling throughout with delays optimized for 15 and 160 Hz, respectively. Triple-resonance experiments were recorded on either an 8 mm inverse $^1H/^{13}C$/BB probe without gradients at 600 MHz or a 5 mm inverse $^1H/^{31}P$/BB Z-gradient probe at 500 MHz.

Mass spectra were obtained at the Australian National University on a VG ZAB 2SEQ instrument (30 kV Cs^+ ions, current 1 mA, accelerating potential 8 kV, matrix 3-nitrobenzyl alcohol). Peaks are reported in the following form: *m*/*z* (assignment, relative intensity). Elemental microanalyses were performed by the Microanalysis Service Unit in the Research School of Chemistry, Australian National University.

Reaction of $Cp_2W_2Ir_2(CO)_{10}$ with 1 Equiv of PPh_3 (Method A). A deep red solution of $Cp_2W_2Ir_2(CO)_{10}$ (20.0 mg, 0.0172 mmol) and PPh_3 (4.5 mg, 0.0175 mmol) in CH_2Cl_2 (20 mL) was stirred at room temperature for 18 h. The red-brown

(6) Waterman, S. M.; Humphrey, M. G.; Tolhurst, V.-A.; Skelton, B. W.; White, A. H. *Organometallics* **1996**, *15*, 934.
(7) Waterman, S. M.; Humphrey, M. G. *Organometallics, in press.*
(8) Shapley, J. R.; Hardwick, S. J.; Foose, D. S.; Stucky, G. D. *J. Am. Chem. Soc.* **1981**, *103*, 7383.
(9) Siegel, J. S.; Anet, F. A. L. *J. Org. Chem.* **1988**, *53*, 2629.
(10) Harris, R. K. In *Nuclear Magnetic Resonance Spectroscopy: A Physicochemical View*; Harris, R. K., Ed.; Pitman: London, 1983; p 230.

solution obtained was evaporated to dryness. The resultant brown residue was dissolved in CH_2Cl_2 (ca. 1 mL) and chromatographed (3/2 CH_2Cl_2/petroleum ether eluant). Two bands were obtained, one in trace amounts. Crystallization of the contents of the second band, R_f 0.42, from CH_2Cl_2/MeOH or CH_2Cl_2/*n*-hexane afforded deep red crystals of $Cp_2W_2Ir_2(\mu\text{-}CO)_3(CO)_6(PPh_3)$ (**2**; 16 mg, 62%). Analytical data for **2**·CH_2Cl_2 are as follows. IR (c-C_6H_{12}): 2041vs, 2023 w, 2002 m, 1987 s, 1980 m, 1958 m, 1921 m, 1840 m cm^{-1}. ^1H NMR ($CDCl_3$, 298 K): δ 7.44−7.37 (m, 15H, Ph), 5.32 (s, 2H, CH_2Cl_2), 4.68 [s (br), 10H, C_5H_5]. ^1H NMR (CD_2Cl_2, 183 K): 7.68−7.05 (m, 15H, Ph), 4.79 (s, 3H, C_5H_5), 4.68 (s, 2H, C_5H_5), 4.40 (s, 3H, C_5H_5), 4.30 (s, 2H, C_5H_5). ^{13}C NMR ($CDFCl_2$, 153 K): **2a**, 248.8 (e; s; 0.6), 227.5 (c; s; 0.6), 221.5 (g; s; 0.6), 215.8 (d; s; 0.6), 211.4 (a or b; s; 0.6), 210.7 (b or a; s; 0.6), 183.9 (h; s; 0.6), 180.1 (f; s; 0.6), 172.7 (i; s; 0.6) ppm; **2b**, 241.4 (E; s; 0.4), 240.9 (C; s; 0.4), 223.9 (G; s; 0.4), 216.7 (D; s; 0.4), 213.0 (A; s; 0.4), 207.5 (B; s; 0.4), 183.3 (F; s; 0.4), 182.2 (H; s; 0.4), 166.8 (I; s; 0.4) ppm. ^{13}C NMR (CD_2Cl_2, 183 K): **2a**, 244.3 (e; s, 85%, d, 15% $^1J_{WC}$ = 81 Hz; 0.6), 224.2 (c; s, 85%, d, 15% $^1J_{WC}$ = 83 Hz; 0.6), 220.3 (g; s, 85%, d, 15% $^1J_{WC}$ = 180 Hz; 0.6), 214.1 (d; s; 0.6), 209.8 (a, b; s, 85%, d, 15% $^1J_{WC}$ = 171 Hz; 1.2), 183.5 (h; s; 0.6), 179.2 (f; d ^2J = 13 Hz; 0.6), 172.2 (i; s; 0.6) ppm; **2b**, 237.7 (E; s, 85%, d, 15% $^1J_{WC}$ = 80 Hz; 0.4), 237.5 (C; s, 85%, d, 15% $^1J_{WC}$ = 80 Hz; 0.4), 222.7 (G; s, 85%, d, 15% $^1J_{WC}$ = 178 Hz; 0.4), 214.1 (D; s; 0.4), 211.3 (A or B; s, 85%, d, 15% $^1J_{WC}$ = 165 Hz; 0.4), 206.1 (B or A; s, 85%, d, 15% $^1J_{WC}$ = 163 Hz; 0.4), 182.4 (F; d, $^2J_{PC}$ = 13 Hz; 0.4), 181.2 (H; s; 0.4), 167.3 (I; s; 0.4) ppm. ^{13}C NMR (CD_2Cl_2, 183 K): 133.0−128.2 (Ph), 88.2 (s, C_5H_5), 87.8 (s, C_5H_5), 87.3 (s, C_5H_5), 85.4 (s, C_5H_5). ^{31}P NMR (CD_2Cl_2, 183 K): 9.2 (0.4P, **2b**), −9.8 (0.6P, **2a**) ppm. MS: 1340 ([M − 2CO]$^+$, 29), 1284 ([M − 3CO]$^+$, 61), 1255 ([M − 4CO]$^+$, 36), 1228 ([M − 5CO]$^+$, 36), 1200 ([M − 6CO]$^+$, 50), 1170 ([M − 7CO]$^+$, 21). Anal. Calcd: C, 30.81; H, 1.84. Found: C, 31.04; H, 1.30.

Reaction of $Cp_2W_2Ir_2(CO)_{10}$ with 2 Equiv of PPh_3. Following method A, $Cp_2W_2Ir_2(CO)_{10}$ (20.0 mg, 0.0172 mmol) and PPh_3 (9.0 mg, 0.0344 mmol) in CH_2Cl_2 (20 mL) afforded one product after chromatography (2/1 CH_2Cl_2/petroleum ether eluant). The band, R_f 0.30, was crystallized (CH_2Cl_2/MeOH at −20 °C) to afford red crystals of $Cp_2W_2Ir_2(\mu\text{-}CO)_3(CO)_5(PPh_3)_2$ (**3**; 9 mg, 32%). Analytical data for **3** are as follows. IR (c-C_6H_{12}): 2041 s, 2024 w, 2003 vs, 1987 m, 1980 vs, 1969 m, 1950 vs, 1921 m, 1909 m, 1896 s, 1850 m, 1803 m cm^{-1}. ^1H NMR (CD_2Cl_2, 203 K): 7.80−7.31 (m, 30H, Ph), 4.68 (s, 5H, C_5H_5, both isomers), 4.55 (s, 4H, C_5H_5, major isomer), 4.42 (s, 1H, C_5H_5, minor isomer). ^{13}C NMR (CD_2Cl_2, 203 K): **3a**, 249.8 (s; 0.2), 238.0 (s; 0.2), 229.9 (s; 0.2), 223.9 (s; 0.2), 214.0 (s; 0.2), 212.9 (s; 0.2), 181.2 (s; 0.2), 158.0 (s; 0.2) ppm; **3b**, 249.1 (s; 0.8), 240.1 (s; 0.8), 226.9 (s; 0.8), 223.1 (s; 0.8), 211.5 (s; 0.8), 210.7 (s; 0.8), 185.0 (s; 0.8), 164.6 (s; 0.8). ^{13}C NMR (CD_2Cl_2, 203 K): 135.0−128.3 (Ph), 88.5 (s, C_5H_5), 87.4 (s, C_5H_5), 87.1 (s, C_5H_5), 85.9 (s, C_5H_5). ^{31}P NMR (CD_2Cl_2, 203 K): 27.3 (s, 0.2P, **3a**), 17.2 (s, 0.8P, **3b**), 8.1 (s, 0.8P, **3b**), 1.9 (s, 0.2P, **3a**) ppm. MS: 1340 ([M − PPh_3 − CO]$^+$, 29), 1311 ([M − PPh_3 − 2CO]$^+$, 10), 1284 ([M − PPh_3 − 3CO]$^+$, 67), 1255 ([M − PPh_3 − 4CO]$^+$, 37), 1228 ([M − PPh_3 − 5CO]$^+$, 38), 1200 ([M − PPh_3 − 6CO]$^+$, 50), 1170 ([M − PPh_3 − 7CO]$^+$, 22), 1142 ([M − PPh_3 − 8CO]$^+$, 40). Satisfactory microanalyses could not be obtained due to sample decomposition at room temperature.

Reaction of $Cp_2W_2Ir_2(CO)_{10}$ with 1 Equiv of PMe_3. Following method A, $Cp_2W_2Ir_2(CO)_{10}$ (21.0 mg, 0.0181 mmol) and PMe_3 (19 μL, 1 M solution in THF, 0.019 mmol) in THF (20 mL) afforded two products after chromatography (3/2 CH_2Cl_2/petroleum ether eluant), one of which was in trace amounts. The major product, R_f 0.45, was crystallized ($CHCl_3$/MeOH) to afford orange crystals of $Cp_2W_2Ir_2(\mu\text{-}CO)_3(CO)_6(PMe_3)$ (**4**; 8.2 mg, 38%). Analytical data for **4** are as follows. IR (c-C_6H_{12}) :2026 s, 2001 w, 1986 vs, 1957 m, 1922 w, 1895 w, 1867 w, 1833 br w cm^{-1}. ^1H NMR ($CDCl_3$, 298 K): δ 4.90 (s, 10H, C_5H_5), 1.87 (d, J_{HP} = 9 Hz, 9H, Me). Major isomer **4b**: ^1H NMR (CD_2Cl_2, 183 K) 4.94 (d, $^4J_{HP}$ = 2 Hz, 5H, C_5H_5), 4.68 (s, 5H, C_5H_5), 1.65 (d, $^2J_{HP}$ = 11 Hz, 9H, Me); ^{13}C NMR (CD_2Cl_2, 183 K) 241.3 (E; s, 85%, d, 15% $^1J_{WC}$ = 71 Hz; 1.0), 239.2 (C; s, 85%, d, 15% $^1J_{WC}$ = 97 Hz; 1.0), 222.4 (G; s, 85%, d, 15% $^1J_{WC}$ = 183 Hz; 1.0), 215.6 (D; s; 1.0), 212.4 (A or B; s, 85%, d, 15% $^1J_{WC}$ = 164 Hz; 1.0), 208.1 (B or A; s, 85%, d, 15% $^1J_{WC}$ = 158 Hz; 1.0), 182.7 (F; d $^2J_{PC}$ = 10 Hz; 1.0), 181.4 (H; s; 1.0), 165.6 (I; s; 1.0) ppm; ^{13}C NMR (CD_2Cl_2, 183 K) 88.4 (s, C_5H_5), 88.0 (s, C_5H_5), 19.6 (d, $^1J_{CP}$ = 37 Hz, Me); ^{31}P NMR (CD_2Cl_2, 183 K) −26.2 (s). Unidentified minor isomer(s): ^1H NMR (CD_2Cl_2, 183 K) 4.87 [s (br)], 1.92 (d, $^2J_{HP}$ = 11 Hz); ^{13}C NMR (CD_2Cl_2, 183 K) 220.0 (s) ppm; ^{31}P NMR (CD_2Cl_2, 183 K) −26.2 (br s) ppm. MS: 1210 ([M]$^+$, 10), 1182 ([M − CO]$^+$, 44), 1154 ([M − 2CO]$^+$, 61), 1126 ([M − 3CO]$^+$, 90), 1098 ([M − 4CO]$^+$, 74), 1070 ([M − 5CO]$^+$, 100), 1042 ([M − 6CO]$^+$, 62). Anal. Calcd: C, 21.83; H, 1.58. Found: C, 21.78; H, 1.65.

Reaction of $Cp_2W_2Ir_2(CO)_{10}$ with 2 Equiv of PMe_3. Following method A, $Cp_2W_2Ir_2(CO)_{10}$ (20.2 mg, 0.0174 mmol) and PMe_3 (18 μL, 1 M solution in THF, 0.038 mmol) in THF (20 mL) afforded two products after chromatography (3/2 CH_2Cl_2/petroleum ether eluant), one of which was in trace amounts. The major product, R_f 0.31, was crystallized ($CHCl_3$/MeOH) to afford orange crystals of $Cp_2W_2Ir_2(\mu\text{-}CO)_3(CO)_5(PMe_3)_2$ (**5**; 9.3 mg, 42%). Analytical data for **5** are as follows. IR (c-C_6H_{12}): 2054 w, 2048 m, 2029 w, 1994 m, 1982 s, 1972 s, 1958 vs, 1948 s, 1873 br m, 1839 m cm^{-1}. ^1H NMR ($CDCl_3$, 298 K): δ 4.78 (s, 10H, C_5H_5), 1.83 (d, J_{HP} = 12 Hz, 18H, Me). ^1H NMR (CD_2Cl_2, 183 K): 4.98 (s, 2H, C_5H_5), 4.87 (s, 3H, C_5H_5), 4.56 (s, 3H, C_5H_5), 4.41 (s, 2H, C_5H_5), 1.94 (d, J_{HP} = 10 Hz, 5.4H, Me), 1.89 (d, J_{HP} = 10 Hz, 3.6H, Me), 1.64 (d, J_{HP} = 10 Hz, 3.6H, Me), 1.54 (d, J_{HP} = 10 Hz, 5.4H, Me). ^{13}C NMR (CD_2Cl_2, 183 K): **5a**, 253.8 (c; s, 85%, d, 15% $^1J_{WC}$ = 90 Hz; 0.60), 242.2 (d; s, 85%, d, 15% $^1J_{WC}$ = 88 Hz; 0.60), 227.6 (e; s; 0.60), 223.0 (h; s, 85%, d, 15% $^1J_{WC}$ = 185 Hz; 0.60), 218.5 (a or b; s, 85%, d, 15% $^1J_{WC}$ = 180 Hz; 0.60), 216.5 (b or a; s, 85%, d, 15% $^1J_{WC}$ = 180 Hz; 0.60), 183.5 (f; dd, $^2J_{PC}$ = 22 Hz, $^3J_{PC}$ = 10 Hz; 0.60), 169.1 (g; d, $^2J_{PC}$ = 10 Hz; 0.60); **5b,** 251.7 (D; s, 85%, d, 15% $^1J_{WC}$ = 92 Hz; 0.35), 247.9 (C; s, 85%, d, 15% $^1J_{WC}$ = 90 Hz; 0.35), 228.1 (E; s; 0.35), 223.0 (H; s, 85%, d, 15% $^1J_{WC}$ = 183 Hz; 0.35), 214.0 (A or B; s, 85%, d, 15% $^1J_{WC}$ = 185 Hz; 0.35), 212.2 (B or A; s, 85%, d, 15% $^1J_{WC}$ = 188 Hz; 0.35), 186.0 (F; dd, $^2J_{PC}$ = 22 Hz, $^3J_{PC}$ = 10 Hz; 0.35), 165.9 (G, d, ^2J = 10 Hz; 0.35); **5c,** 244.9 (*c* or *d*; s; 0.05), 228.2 (*e*; s; 0.05), 221.3 (*h*; s; 0.05), 215.9 (*a* or *b*; s; 0.05), 167.2 (*f* or *g*; d $^2J_{PC}$ = 10 Hz; 0.05), 163.8 (*g* or *f*; d, $^2J_{PC}$ = 10 Hz; 0.05), other signals not observed. ^{13}C NMR (CD_2Cl_2, 183 K): 89.2 (s, C_5H_5), 88.4 (s, C_5H_5), 87.9 (s, C_5H_5), 87.5 (s, C_5H_5), 20.5 (d, $^1J_{CP}$ = 35 Hz, Me), 19.3 (d, $^1J_{CP}$ = 35 Hz, Me), 17.7 (d, $^1J_{CP}$ = 35 Hz, Me). ^{31}P NMR (CD_2Cl_2, 183 K): −47.7 (s, 0.60P, **5a**), −29.8 (s, 0.35P, **5b**), −28.5 (d ^3J = 10 Hz, 0.05P, **5c**), −27.7 (s, 0.35P, **5b**), −19.4 (s, 0.60P, **5a**), −17.2 (d ^3J = 10 Hz, 0.05P, **5c**) ppm. MS: 1258 ([M]$^+$, 11), 1230 ([M − CO]$^+$, 12), 1202 ([M − 2CO]$^+$, 76), 1174 ([M − 3CO]$^+$, 95), 1146 ([M − 4CO]$^+$, 100), 1118 ([M − 5CO]$^+$, 83). Satisfactory microanalyses could not be obtained due to sample decomposition over a number of days.

X-ray Crystallography. Crystals of compound **2a** suitable for diffraction analyses were grown by slow diffusion of hexane into a dichloromethane solution at room temperature. A unique diffractometer data set was measured at ~295 K within the specified $2\theta_{max}$ limit ($2\theta/\theta$ scan mode; monochromatic Mo Kα radiation (λ = 0.710 7$_3$ Å)), yielding N independent reflections. N_o of these with $I > 3\sigma(I)$ were considered "observed" and used in the full-matrix/large-block least-squares refinements after analytical absorption correction. Anisotropic thermal parameters were refined for the non-hydrogen atoms; $(x, y, z, U_{iso})_H$ were included, constrained at estimated values. Conventional residuals R, R_w on $|F|$ at convergence are given. Neutral atom complex scattering factors were used, the computation using teXsan.[11] Pertinent results are given in Figure 2 and Tables 1 and 2. Atomic coordinates, bond lengths and angles, and

thermal parameters have been deposited at the Cambridge Structural Database and in the Supporting Information.

Results

Syntheses and Characterization. The reactions of $Cp_2W_2Ir_2(CO)_{10}$ (**1**) with *n* equivalents of PPh_3 and PMe_3 ($n = 1, 2$) proceeded in dichloromethane at room temperature to afford the clusters $Cp_2W_2Ir_2(\mu\text{-}CO)_3(CO)_{7-n}(PPh_3)_n$ ($n = 1$ (**2**), 2 (**3**)) and $Cp_2W_2Ir_2(\mu\text{-}CO)_3(CO)_{7-n}(PMe_3)_n$ ($n = 1$ (**4**), 2 (**5**)), respectively, as the major or sole reaction products in good to excellent yields (38−63%). The bis(triphenylphosphine)-substituted product $Cp_2W_2Ir_2(\mu\text{-}CO)_3(CO)_5(PPh_3)_2$ (**3**) was found to be unstable above 273 K; workup of the reaction between **1** and 2 equiv of PPh_3 revealed that decomposition of **3** occurred on the thin-layer chromatographic plate to afford **2**, but a swift workup afforded sufficient **3** to permit spectroscopic characterization. The products were characterized by a combination of IR and ^1H, ^{13}C, and ^{31}P NMR spectroscopy, mass spectrometry, and satisfactory microanalyses for the mono(phosphine) clusters. Infrared spectra suggest the presence of edge-bridging carbonyl ligands in all complexes (ν(CO) 1840−1803 cm^{-1}), which contrasts with the all-terminal geometry of the precursor **1**. In combination with the X-ray structural results detailed below, the numbers of bands in the terminal carbonyl ligand ν(CO) regions of the IR spectra are indicative of the presence of isomers. The ^1H NMR spectra contain signals assigned to cyclopentadienyl and phenyl groups for **2** and **3** and cyclopentadienyl and methyl groups for **4** and **5**, in the appropriate ratios. Discussion of the ^{13}C and ^{31}P NMR spectra is deferred until the solid-state structure is presented (see below). The mass spectra of the complexes **4** and **5** contain molecular ions, and all complexes contain fragment ions corresponding to stepwise loss of carbonyls; isotope patterns are consistent with the presence of two iridium atoms and two tungsten atoms.

X-ray Structural Study of 2a. The molecular structure of **2a** as determined by a single-crystal X-ray study is consistent with the formulation given above and defines the substitution site of the phosphine. A summary of crystal and refinement data is shown in Table 1, and selected bond distances and angles are listed in Table 2. Figure 2 contains an ORTEP plot showing the molecular geometry and atomic numbering scheme.

Complex **2a** has the pseudotetrahedral framework of the precursor cluster **1**.[12] Each tungsten atom bears one η^5-cyclopentadienyl group, and three bridging carbonyls span a WIr_2 face. Six terminal carbonyl ligands and an iridium-ligated triphenylphosphine ligand complete the coordination sphere. The W_2Ir_2 core distances ($W-Ir_{av}$ = 2.866 Å, W−W = 3.0604(6) Å, Ir−Ir = 2.7348(6) Å) are all slightly longer than those of **1** ($W-Ir_{av}$ = 2.835 Å, W−W = 2.991(1) Å, Ir−Ir = 2.722(1) Å); core distances of the related mono(phosphine)-substituted tungsten−triiridium clusters $CpWIr_3(\mu\text{-}CO)_3(CO)_7(L)$ (L = PPh_3, PMe_3,[6] PMe_2Ph[13]) compared to those of the precursor $CpWIr_3(CO)_{11}$ are also consistent with core expansion upon introduction of P-donor ligands. Intracore bond angles are all close to 60° as expected. As was observed with **1**, angles centered at iridium for **2a** are slightly larger (60.01(2)−64.78(2)°) than those centered at tungsten (56.66(1)−59.08(1)°). The Ir−P distance (2.3483(3) Å) and intraphosphine bond lengths and angles are not unusual. With respect to the plane of bridging carbonyls, PPh_3 occupies an axial coordination site with the cyclopentadienyl groups in axial and apical positions. Formal electron counting ((2 × 6 (W)) + (2 × 9 (Ir)) + (2 × 5 (Cp)) + (9 × 2 (CO)) + (2 (PPh_3))) reveals that **2a** has 60 e, electron precise for a tetrahedral cluster.

Table 1. Crystallographic Data for 2a

formula	$C_{37}H_{25}Ir_2O_9PW_2 \cdot CH_2Cl_2$
fw	1481.65
space group	$P\bar{1}$ (No. 2)
cryst syst	triclinic
a (Å)	8.879 (2)
b (Å)	13.098(3)
c (Å)	17.539(2)
α (deg)	105.99(1)
β (deg)	95.26(1)
γ (deg)	101.05(2)
V (Å^3)	1901.7(6)
ρ_{calcd} (g cm^{-3})	2.587
Z	2
μ (mm^{-1})	13.3
specimen size (mm^3)	0.52 × 0.28 × 0.12
A (min, max)	0.24, 1.00
$2\theta_{max}$ (deg)	50.1
N	6750
N_o	5360
R	0.032
R_w	0.033

Table 2. Important Bond Lengths (Å) and Angles (deg) for 2a

Ir(1)−Ir(2)	2.7348(6)	Ir(1)−W(3)	2.8294(7)
Ir(1)−W(4)	2.8833(6)	Ir(2)−W(3)	2.9146(6)
Ir(2)−W(4)	2.8381(6)	W(3)−W(4)	3.0604(6)
Ir(2)−P(1)	2.348(3)	Ir(1)−C(11)	1.88(1)
Ir(1)−C(12)	2.13(1)	Ir(1)−C(13)	2.25(1)
Ir(2)−C(12)	2.07(1)	Ir(2)−C(21)	1.83(1)
Ir(2)−C(23)	2.11(1)	W(3)−C(13)	2.08(1)
W(3)−C(23)	2.25(1)	W(3)−C(31)	1.94(1)
W(3)−C(301)	2.29(1)	W(3)−C(302)	2.32(1)
W(3)−C(303)	2.30(1)	W(3)−C(304)	2.28(1)
W(3)−C(305)	2.30(1)	W(4)−C(41)	1.98(1)
W(4)−C(42)	1.98(1)	W(4)−C(401)	2.28(1)
W(4)−C(402)	2.31(1)	W(4)−C(403)	2.37(1)
W(4)−C(404)	2.39(1)	W(4)−C(405)	2.31(1)
Ir(2)−Ir(1)−W(3)	63.15(1)	Ir(2)−Ir(1)−W(4)	60.62(1)
W(3)−Ir(1)−W(4)	64.78(2)	Ir(1)−Ir(2)−W(3)	60.01(2)
Ir(1)−Ir(2)−W(4)	62.28(1)	W(3)−Ir(2)−W(4)	64.26(1)
Ir(1)−W(3)−Ir(2)	56.84(2)	Ir(1)−W(3)−W(4)	58.46(1)
Ir(2)−W(3)−W(4)	56.66(1)	Ir(1)−W(4)−Ir(2)	57.10(1)
Ir(1)−W(4)−W(3)	56.76(1)	Ir(2)−W(4)−W(3)	59.08(1)
Ir(1)−Ir(2)−P(1)	118.74(7)	W(3)−Ir(2)−P(1)	113.01(6)
W(4)−Ir(2)−P(1)	176.49(6)		

NMR Spectra of $Cp_2W_2Ir_2(\mu\text{-}CO)_3(CO)_6(PMe_3)$ (4). The room-temperature ^{31}P NMR spectrum of **4** in CD_2Cl_2 consists of a broad singlet at −26.8 ppm (Figure 3). When the temperature is lowered to 183 K, one sharp signal at −26.2 ppm and a very broad singlet at −20.3 ppm are resolved, in the approximate ratio 4:1. Similarly, the ^{13}C NMR spectrum of **4** at 298 K (Figure 4) shows a single broad resonance at 205.3 ppm, but at 183 K the fluxional processes are sufficiently slow to distinguish the nine carbonyl resonances of **4**, with one signal at 220.0 ppm belonging to (an) isomer(s) under-

(11) teXsan: Single-Crystal Structure Analysis Software, Version 1.7-3; Molecular Structure Corp., The Woodlands, TX, 1995.

(12) Churchill, M. R.; Bueno, C.; Hutchinson, J. P. *Inorg. Chem.* **1982**, *21*, 1359.

(13) Waterman, S. M.; Humphrey, M. G.; Hockless, D. C. R. *J. Organomet. Chem.* **1998**, *565*, 81.

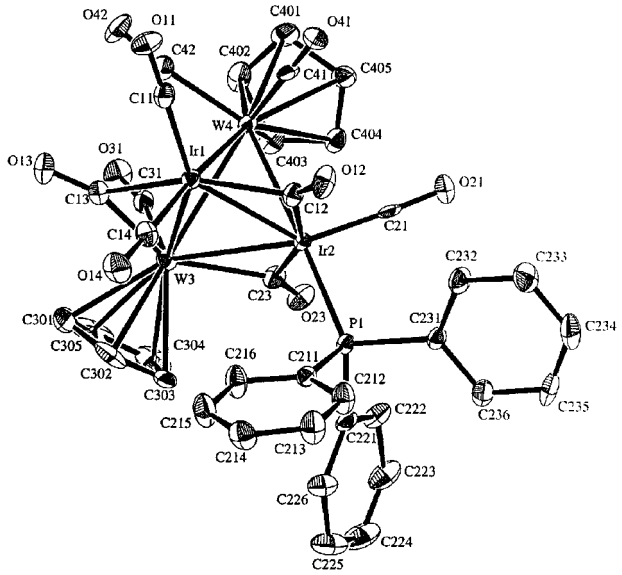

Figure 2. Molecular structure and atomic labeling scheme for $Cp_2W_2Ir_2(\mu\text{-}CO)_3(CO)_6(PPh_3)$ (**2a**). Thermal envelopes at the 20% level are shown for the non-hydrogen atoms; hydrogen atoms have arbitrary radii of 0.1 Å.

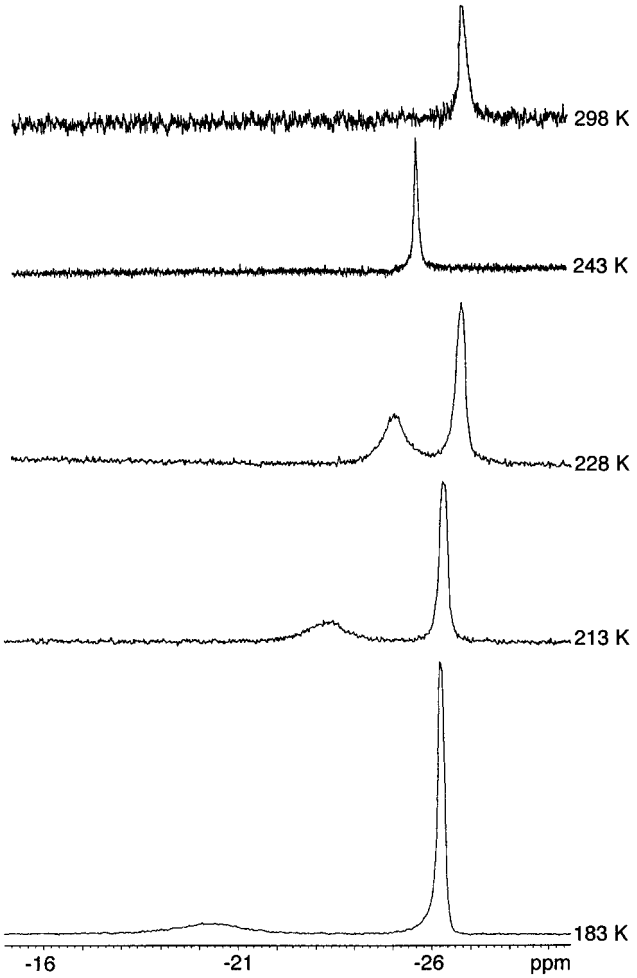

Figure 3. Variable-temperature ^{31}P NMR spectroscopic study of $Cp_2W_2Ir_2(\mu\text{-}CO)_3(CO)_6(PMe_3)$ (**4**) in CD_2Cl_2 at 121.4 MHz.

going very fast exchange, presumably correlated with the broad phosphorus resonance at −20.3 ppm. These broad signals could not be resolved into constituent

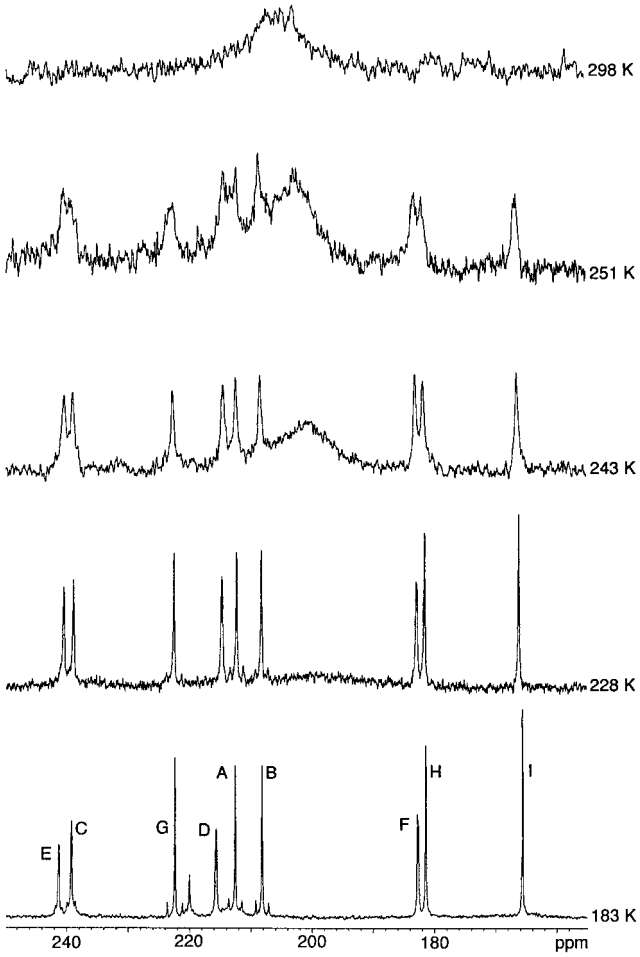

Figure 4. Variable-temperature ^{13}C NMR spectroscopic study of $Cp_2W_2Ir_2(\mu\text{-}CO)_3(CO)_6(PMe_3)$ (**4**) in CD_2Cl_2 at 75.4 MHz.

isomers to the freezing points of the solvents utilized. The proposed configuration of **4**, with axial phosphine, radial Cp, and apical Cp, has been assigned utilizing information from the ^{13}C NMR spectrum, a HSQC experiment (Figure 5), and a triple-resonance $^1H-^{31}P-^{13}C$ experiment (Figure 6). $^1H-^{31}P-^{13}C$ triple-resonance experiments were acquired using the pulse sequence shown in Figure 1. The experiment consists of an initial INEPT transfer from ^1H to ^{31}P followed by creation of a two-spin $^{31}P-^{13}C$ coherence with ^{13}C frequency labeling and a final reverse transfer INEPT transfer from ^{31}P to ^1H. In terms of coherence transfer, this experiment is, in essence, the same as a reduced dimensionality version of early implementations of the 3D HNCO experiment[14] used in the determination of protein structures. As a result, the term 2D HPCO experiment is required to determine through which phosphorus the carbon information was relayed in these experiments. The information obtained from the HPCO experiment is basically the same as can be extracted from 2D $^{31}P-^{13}C\{^1H\}$ experiments which have been employed in the literature.[15] However, greater sensitivity is obtained using the double INEPT transfer to and from ^{31}P from ^1H. The PMe_3 ligand, with nine protons per phosphorus, is particularly well-suited to these experiments, since

(14) Kay, L. E.; Ikura, M.; Tschudin, R.; Bax, A. *J. Magn. Reson.* **1990**, *89*, 496.
(15) López-Ortiz, F.; Carbajo, R. *J. Curr. Org. Chem.* **1998**, *2*, 97.

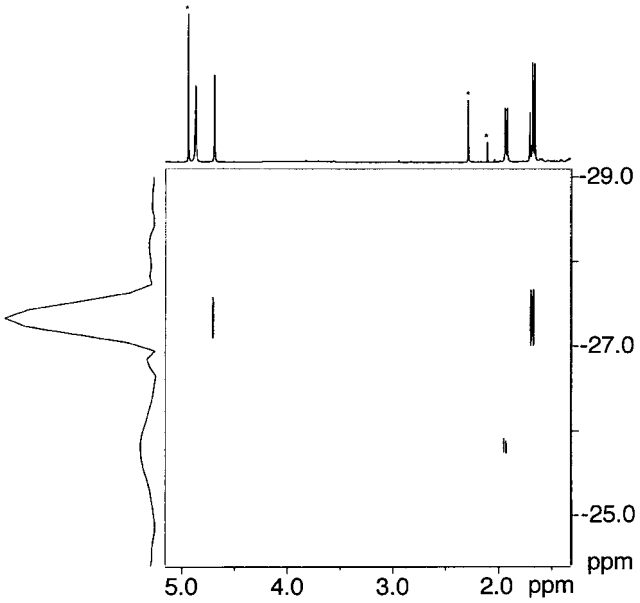

Figure 5. HSQC NMR spectrum of $Cp_2W_2Ir_2(\mu\text{-}CO)_3(CO)_6(PMe_3)$ (**4**) in CD_2Cl_2 at 203 K at 500.13 (^{1}H) MHz.

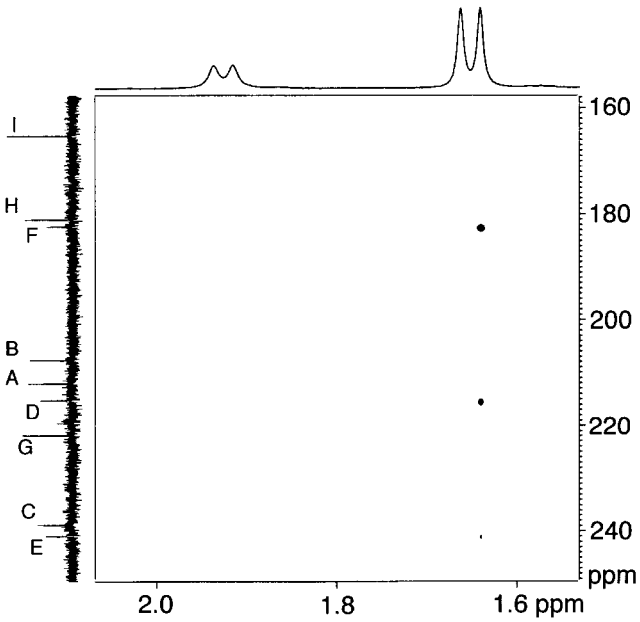

Figure 6. Triple-resonance ^{1}H−^{31}P−^{13}C NMR spectroscopic study of $Cp_2W_2Ir_2(\mu\text{-}CO)_3(CO)_6(PMe_3)$ (**4**) in CD_2Cl_2 at 203 K at 500.13 (^{1}H) MHz.

the ^{1}H resonance is a simple doublet due to phosphorus coupling. With PPh_3, the presence of homonuclear couplings, $^3J_{HH}$, of similar magnitude to $^3J_{HP}$ complicates the coherence transfer and a simpler 2D ^{31}P−^{13}C-{^{1}H} HMQC approach is more easily implemented.[16]

The presence of at least one carbonyl resonance in the bridging carbonyl region and only one carbonyl resonance at high field in the apical/axial region excludes both an all-terminal ligand configuration and the possibility of a W_2Ir basal plane. This isomer must therefore have a WIr_2 basal plane. There are two Ir-ligated axial sites, but only one is occupied by carbonyl;

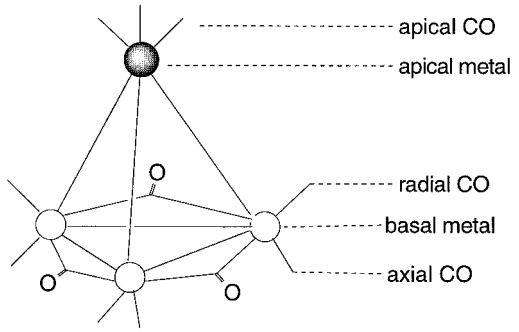

Figure 7.

therefore, the other must be occupied by phosphine. There are six possible configurations which are consistent with this information, corresponding to differing sites for the Cp ligands: the apical Cp ligand can appear over any of the three nonbasal faces, and the basal Cp can be axial or radial (Figure 8). The ^{1}H−^{31}P HSQC experiment of **4** at 213 K in CD_2Cl_2 (Figure 5) reveals a cross-peak between the apical Cp signal at 4.69 ppm in the ^{1}H NMR and the axial PMe_3 signal at −27.3 ppm in the ^{31}P NMR spectra, corresponding to a trans coupling from the protons on the apical Cp to the phosphorus of the PMe_3 ligand. The apical Cp is therefore inclined over the $W_2\{Ir(CO)_2\}$ face. The remaining ambiguity is the basal Cp, which can be radially or axially disposed. A ^{1}H NOESY experiment of **4** in CD_2Cl_2 at 183 K reveals the presence of through-space interactions between the protons on the basal cyclopentadienyl ligand of **4** at 4.94 ppm and the protons on the axially ligating PMe_3 at 1.65 ppm, combined with an absence of through-space interactions between the apical Cp signal at 4.68 ppm and the axial PMe_3 signal at 1.65 ppm; these data strongly suggest that the basal Cp is axially ligating. Furthermore, thermodynamic considerations suggest that the basal Cp should be axially ligated to minimize interligand repulsion with the apical Cp (Figure 8, configuration **4b**). It is significant that this configuration has previously been seen in the structurally characterized $Cp_2Mo_2Ir_2(\mu\text{-}CO)_3(CO)_6(PMe_3)$[17] (Figure 8). We have extended the NMR chemical shift positional sequence established with tetrairidium clusters (bridging > radial > axial ≈ apical[18]) to the mixed-metal regime, affording the chemical shift sequence W−W bridging CO > W−Ir bridging CO > Ir−Ir bridging CO ≈ W terminal CO > Ir radial CO > Ir axial CO ≈ Ir apical CO; it is possible to distinguish Ir−Ir bridging CO's from W terminal CO's due to the 15% abundant ^{183}W-coupled satellites of the latter.[7,13] With this information, it is possible to assign the spectrum of **4**, which consists of nine signals of equivalent intensity at 183 K. ^{183}W-coupled satellites are observed for the resonances at 241.3 (E, 71 Hz), 239.2 (C, 97 Hz), 222.4 (G, 183 Hz), 212.5 (A or B, 164 Hz), and 208.1 ppm (B or A, 158 Hz), the assignments following logically from (i) coupling between the axial phosphine and E rather than C observed in the triple-resonance experiment (Figure 6) and (ii) our earlier observation[7] that coupling constants for terminal car-

(16) Bast, P.; Berger, S.; Günther, H. *Magn. Reson. Chem.* **1992**, *30*, 587.

(17) Lucas, N. T.; Humphrey, M. G.; Healy, P. C.; Williams, M. L. *J. Organomet. Chem.* **1997**, *545*, 519.

(18) Ros, R.; Scrivanti, A.; Albano, V. G.; Braga, D. *J. Chem. Soc., Dalton Trans.* **1986**, 2411.

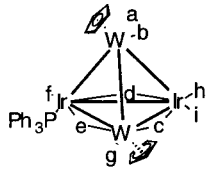

$Cp_2W_2Ir_2(\mu\text{-}CO)_3(CO)_6(PPh_3)$ **2a** XRS
axial PPh_3, axial Cp, apical Cp

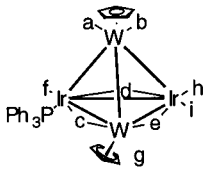

Alternative configuration consistent
with spectral data of **2a** (**2c**)
axial PPh_3, radial Cp, apical Cp

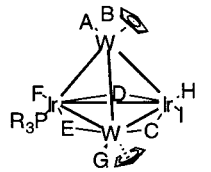

$Cp_2W_2Ir_2(\mu\text{-}CO)_3(CO)_6(PPh_3)$ **2b**
$Cp_2W_2Ir_2(\mu\text{-}CO)_3(CO)_6(PMe_3)$ **4b**
[XRS $Cp_2Mo_2Ir_2(\mu\text{-}CO)_3(CO)_6(PMe_3)$ [a]]
axial PR_3, axial Cp, apical Cp

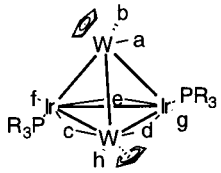

$Cp_2W_2Ir_2(\mu\text{-}CO)_3(CO)_5(PMe_3)_2$ **5a**
axial PMe_3, radial PMe_3, axial Cp, apical Cp

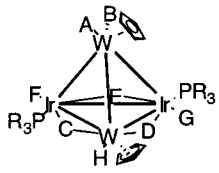

$Cp_2W_2Ir_2(\mu\text{-}CO)_3(CO)_5(PMe_3)_2$ **5b**
[XRS $Cp_2W_2Ir_2(\mu\text{-}CO)_3(CO)_5\{P(OMe)_3\}_2$ [b]]
axial PMe_3, radial PMe_3, axial Cp, apical Cp

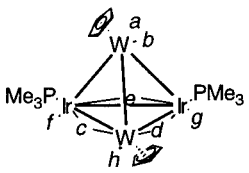

$Cp_2W_2Ir_2(\mu\text{-}CO)_3(CO)_5(PMe_3)_2$ **5c**
diradial PMe_3, axial Cp, apical cp

Figure 8. Isomers of $Cp_2W_2Ir_2(\mu\text{-}CO)_3(CO)_{7-n}(L)_n$ (L = PPh_3, PMe_3; n = 1, 2). Legend: XRS, X-ray study exists; a, ref 17; b, ref 24.

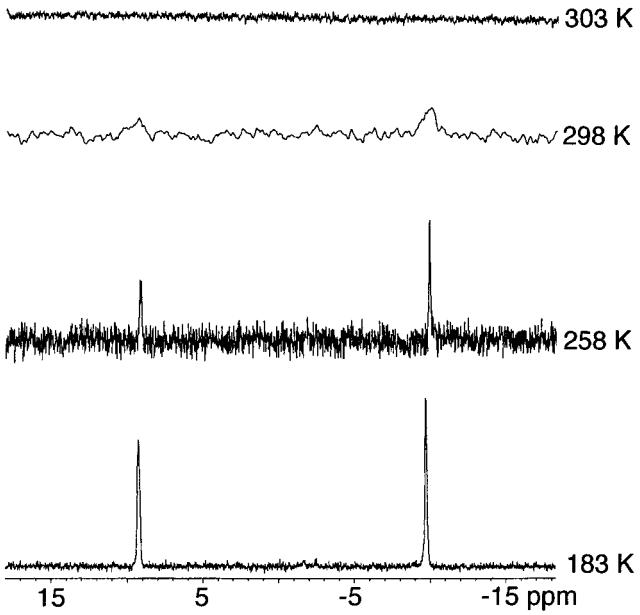

Figure 9. Variable-temperature ^{31}P NMR spectroscopic study of $Cp_2W_2Ir_2(\mu\text{-}CO)_3(CO)_6(PPh_3)$ (**2**) in CD_2Cl_2 at 121.4 MHz.

bonyls are significantly larger than those for bridging carbonyls. Regarding (i), we have noted a similar μ-CO−axial CO coupling in a $^{13}C-^{13}C$ correlation study of $CpWIr_3(\mu\text{-}CO)_3(CO)_6(PPh_3)_2$.[7] Assignment of the remaining signals at 215.6 (D), 182.7 (F, J_{CP} = 10 Hz), 181.4 (H), and 165.6 ppm (I) is straightforward because of the cis coupling observed at carbonyl F.

NMR Spectra of $Cp_2W_2Ir_2(\mu\text{-}CO)_3(CO)_6(PPh_3)$ (2). The ^{31}P NMR spectrum of **2** at 303 K is near coalescence. When the temperature is lowered to 183 K, two signals are resolved in the ratio of 3:2 (Figure 9). Similarly, the ^{13}C NMR spectrum of **2** at 298 K reveals the presence of two average carbonyl signals, whereas cooling to 153 K resolves signals corresponding to the presence of two isomers in the ratio of 3:2 (Figure 10). A broad signal at 221.5 ppm, observed in some preparations, suggests the presence of a minor unidentifiable species, which could not be resolved down to the freezing point of $CDFCl_2$ (Figure 10a). The structures of the two resolvable isomers of **2** can be assigned from the ^{13}C NMR data. The minor isomer **2b** has a set of resonances in the ^{13}C NMR spectrum similar to that observed with **4**, and all resonances are assigned analogously. As with **4**, the presence of only one high-field resonance confirms a configuration with a WIr_2 basal plane and an axially ligated phosphine (9.2 ppm). The spectrum at 183 K reveals ^{183}W-coupled satellites for the resonances at 237.7 (E or C, 80 Hz), 237.5 (C or E, 80 Hz), 222.7 (G, 178 Hz), 211.3 (A, 165 Hz), and 206.1 ppm (B, 163 Hz), together with signals at 214.1 (D), 182.4 (F, J_{CP} = 13 Hz), 181.2 (H) and 167.3 ppm (I), with the only ambiguity being the assignment of E and C (it is assumed that carbonyl A resonates 4−5 ppm downfield of carbonyl B, as observed in **4**).

The major isomer, **2a**, almost certainly corresponds to the crystallographically characterized form. As with **2b** and **4**, the presence of at least one carbonyl resonance in the bridging carbonyl region and only one carbonyl resonance at high field in the apical/axial region of **2a** exclude both an all-terminal ligand configuration and the possibility of a W_2Ir basal plane for either isomer; **2a** must therefore have a WIr_2 basal plane. As with **2b** and **4**, there are two Ir-ligated axial sites, but only one is occupied by carbonyl; the other must therefore be occupied by phosphine (^{31}P NMR −9.8 ppm). As mentioned above with **2b** and **4**, there are six possible configurations which are consistent with this information, corresponding to differing sites for the Cp ligands: the apical Cp ligand can appear over any of the three nonbasal faces, and the basal Cp can be axial or radial. Steric considerations militate against a radial Cp when the apical Cp is inclined to either W_2Ir face; in these circumstances axial Cp is favored. As with **4**, a ^1H NOESY experiment of **2** in CD_2Cl_2 at 183 K shows the presence of a cross-peak between the axial PPh_3

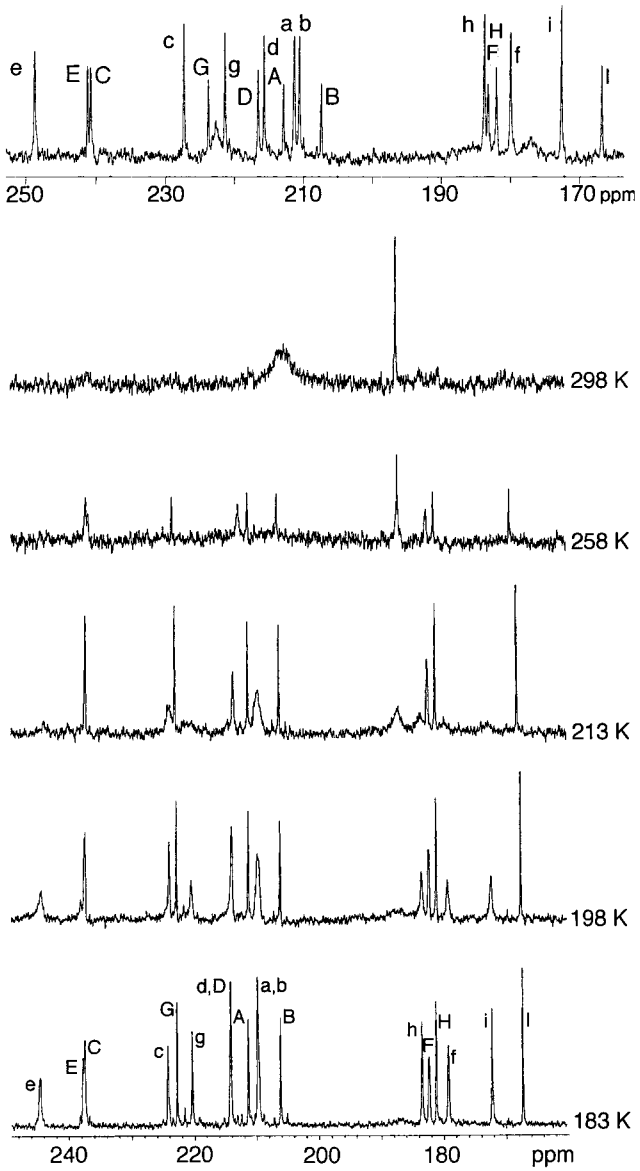

Figure 10. (a, top) ^{13}C NMR spectrum of $Cp_2W_2Ir_2(\mu\text{-}CO)_3(CO)_6(PPh_3)$ (**2**) in $CDFCl_2$ at 153 K at 125.7 MHz. (b, bottom) Variable-temperature ^{13}C NMR spectroscopic study of $Cp_2W_2Ir_2(\mu\text{-}CO)_3(CO)_6(PPh_3)$ (**2**) in CD_2Cl_2 at 75.4 MHz.

protons at 7.68−7.05 ppm and the signal assigned to the protons of the axially ligating Cp for **2a** at 4.79 ppm, suggesting an axial phosphine, axial Cp, apical Cp coordination geometry. These two configurations are **2a** and **2b** in Figure 8. The other two possibilities which are not sterically disfavored have apical Cp inclined to the nonbasal WIr_2 face. On steric grounds, the basal Cp can be radial or axial. We have previously noted that an all-trans CpWWCp arrangement is disfavored on electronic grounds.[19] The remaining possibility (radial Cp, axial phosphine, apical Cp) depicted in Figure 8 (**2c**) cannot be excluded on steric or electronic grounds, but the NOESY results as well as the significant difference in chemical shift of the W−Ir(μ-CO) resonances suggest that **2a** is the configuration observed for the major isomer (we have previously noted a significant (>10 ppm) difference between the chemical shift of the bridging carbonyl at the face to which the apical Cp is inclined, when this face also contains two large axial ligands, and that of the other bridging carbonyl[13]). The resonance at 244.3 ppm for the major isomer **2a** therefore corresponds to a W−Ir bridging carbonyl at a face to which the apical Cp is inclined, and which contains axially coordinated phosphine and cyclopentadienyl ligands. Isomer **2a** thus adopts the axial phosphine, axial Cp, apical Cp configuration seen in the solid-state study (Figure 8). The spectrum at 193 K reveals ^{183}W-coupled satellites for the resonances at 244.3 (e, 81 Hz), 224.2 (c, 83 Hz), 220.3 (g, 180 Hz), and 209.8 ppm (a and b, 171 Hz), the assignments for which follow logically from the fact that terminal carbonyl coupling constants are significantly larger than those for bridging carbonyls. The coincident signals for carbonyls a and b are resolved in the spectrum in $CDFCl_2$ at 153 K (Figure 10a), and a $^{31}P-^{13}C$ HMQC study at 173 K shows a correlation between the axial phosphine and one of the apical CO resonances at 210.8 ppm, which is assigned as b, assuming a linear three-bond relationship will give rise to the larger J coupling. Assignment of the remaining signals at 214.1 (d), 183.5 (h), 179.2 (f, J_{CP} = 13 Hz), and 172.2 ppm (i) is straightforward because of the cis coupling observed at carbonyl f.

NMR Spectra of $Cp_2W_2Ir_2(\mu\text{-}CO)_3(CO)_5(PMe_3)_2$ (5). The coalescence point in the NMR spectra of **5** could not be reached due to decomposition of the cluster above 300 K. The room-temperature ^{31}P NMR spectrum of **5** consists of two signals in the ratio 1:1 at −27.7 and −29.8 ppm and a very broad resonance. When the temperature is lowered to 193 K, six signals are resolved, corresponding to three isomers in the ratio 20:12:1 in CD_2Cl_2 (Figure 11). Similarly, when the ^{13}C NMR spectrum of **5** is measured at 193 K, signals corresponding to three isomers in the ratio 20:12:1 in CD_2Cl_2 can be identified (Figure 12). The structures of two of the three isomers of **5** (Figure 7) can be assigned from the ^{13}C NMR data. Isomer **5a**, the most abundant in CD_2Cl_2, contains eight signals of equivalent intensity. The carbonyl resonances in the W−Ir(μ-CO) region and the single resonance in the apical/axial region indicate a WIr_2 basal plane. There are two Ir-ligated axial sites, one occupied by carbonyl, the other occupied by phosphine. The lack of $^{31}P-^{31}P$ and $^{31}P-^{183}W$ coupling is only consistent with the second phosphine occupying a radial site at the axial carbonyl ligated iridium atom. Six configurations corresponding to the differing Cp locations are consistent with these data. A $^{1}H-^{31}P-^{13}C$ triple-resonance experiment reveals a cross-peak between the axial phosphine and an apical carbonyl (Figure 13); the apical Cp is thus located inclined to the $W_2Ir(P_{ax})$ or WIr_2 face. There are four remaining possible configurations (the basal Cp may be radial or axial), but the low-field signal at 253.8 ppm (which shows a cross-peak to the axial PMe_3 in the $^{1}H-^{31}P-^{13}C$ triple-resonance experiment; Figure 13) is significantly downfield of the other W−Ir(μ-CO) resonance and is thus indicative of a carbonyl bridging a bond between two axially ligated metals, with an apical Cp ligand inclined over the resultant face; configuration **5a** (Figure 8) is therefore the only remaining possibility. A ^{1}H NOESY experiment of **5** in CD_2Cl_2 at 183 K reveals a

(19) Waterman, S. M.; Humphrey, M. G.; Hockless, D. C. R. *J. Organomet. Chem.*, in press.

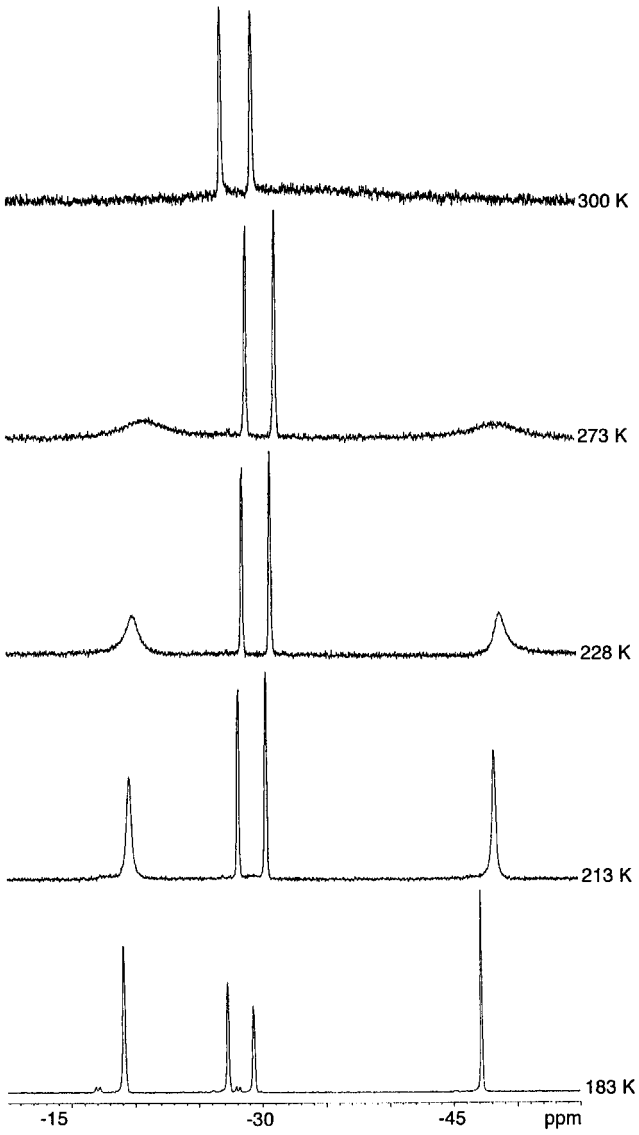

Figure 11. Variable-temperature ^{31}P NMR spectroscopic study of $Cp_2W_2Ir_2(\mu\text{-}CO)_3(CO)_5(PMe_3)_2$ (**5**) in CD_2Cl_2 at 121.4 MHz.

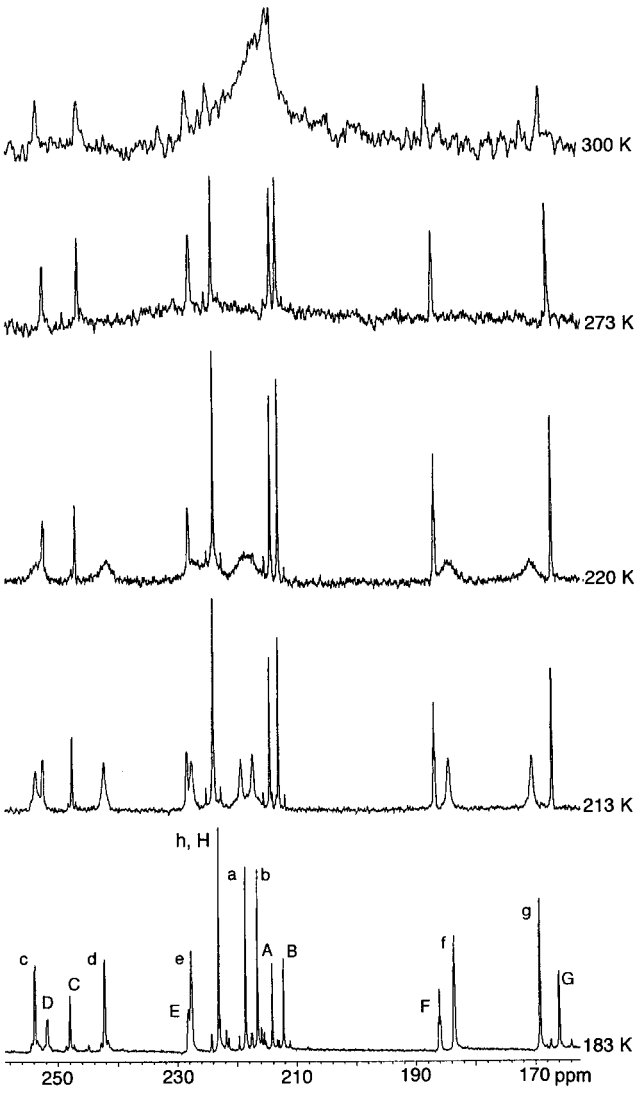

Figure 12. Variable-temperature ^{13}C NMR spectroscopic study of $Cp_2W_2Ir_2(\mu\text{-}CO)_3(CO)_5(PMe_3)_2$ (**5**) in CD_2Cl_2 at 75.4 MHz.

cross-peak between the signal at 4.87 ppm corresponding to the protons on the axially ligating Cp and the signal at 1.54 ppm corresponding to the axially ligating PMe_3 protons, strengthening this assignment. This radial, diaxial, apical geometry is the only configuration structurally characterized thus far (for monodentate ligands) with tetrasubstituted tetrairidium clusters.[20,21] The ^{13}C NMR spectrum at 183 K reveals ^{183}W-coupled satellites for the resonances at 253.8 (c, 90 Hz), 242.2 (d, 88 Hz), 223.0 (h, 185 Hz), 218.5 (a or b, 180 Hz), and 216.5 ppm (b or a, 180 Hz), with the assignments following from (i) coupling constant magnitude, (ii) the $a-P_{ax}$ cross-peak in the triple resonance study (see above), and (iii) the cross-peak between c and P_{ax} in the triple-resonance study (see above). Assignment of the remaining signals at 227.6 (e), 183.5 (f, $^2J_{PC} = 22$ Hz, $^3J_{PC} = 10$ Hz), and 169.1 ppm (g, $^2J_{PC} = 10$ Hz) is straightforward because of the cis and trans coupling to the phosphines.

Isomer **5b** contains eight signals of equivalent intensity and must also possess a WIr_2 basal plane with one phosphine axially ligated and the other radially disposed. A $^1H-^{31}P$ HSQC experiment reveals a cross-peak between the axial phosphine and the apical cyclopentadienyl (Figure 14); the apical Cp is thus located inclined to the $W_2Ir(P_{rad})$ face. There are two remaining possible configurations (the basal Cp may be radial or axial), but a radially disposed basal Cp is highly unlikely on steric grounds, suggesting that configuration **5b** in Figure 8 is correct. The configuration of **5b** is strengthened by the presence of through-space interactions, revealed in the ^1H NOESY experiment at 183 K. A cross-peak between the signal at 4.41 ppm, assigned to the apical Cp protons, and the signal at 1.89 ppm, assigned to the radially ligating PMe_3 protons, strengthens the suggestion that the apical Cp is inclined to the $W_2Ir(P_{rad})$ face. Significantly, we have recently structurally characterized the bis-$P(OMe)_3$ analogue with this configuration (Figure 8). The ^{13}C NMR spectrum at 183 K reveals ^{183}W-coupled satellites for the resonances at

(20) Darensbourg, D. J.; Baldwin-Zuschke, B. J. *Inorg. Chem.* **1981**, *20*, 3846.
(21) Blake, A. J.; Osborne, A. G. *J. Organomet. Chem.* **1984**, *260*, 227.

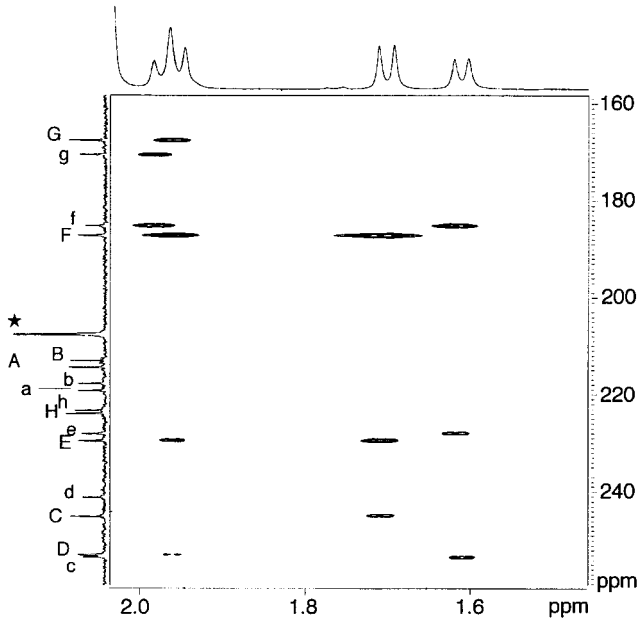

Figure 13. Triple-resonance $^{1}H-^{31}P-^{13}C$ NMR spectrum of $Cp_2W_2Ir_2(\mu\text{-}CO)_3(CO)_5(PMe_3)_2$ (**5**) in acetone-d_6 at 203 K at 600.13 (^{1}H) MHz.

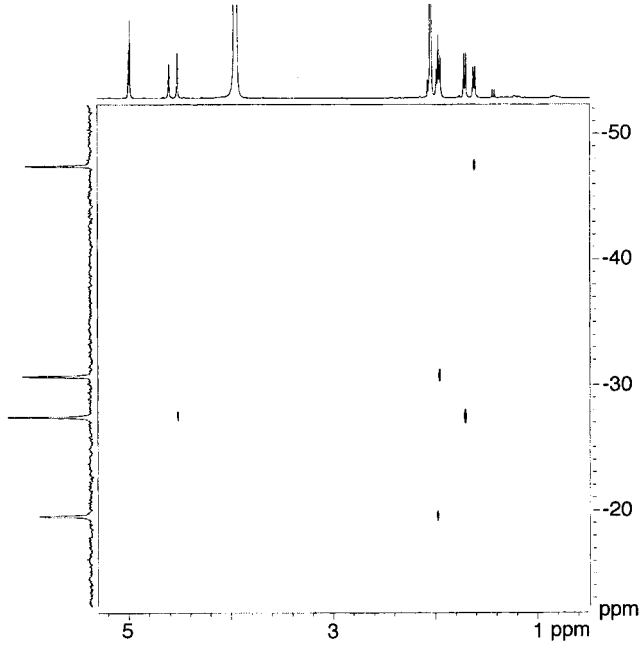

Figure 14. HSQC NMR spectrum of $Cp_2W_2Ir_2(\mu\text{-}CO)_3(CO)_5(PMe_3)_2$ (**5**) in acetone-d_6 at 203 K at 600.13 (^{1}H) MHz.

251.7 (D, 92 Hz), 247.9 (C, 90 Hz), 223.0 (H, 183 Hz), 214.0 (A or B, 185 Hz), and 212.2 ppm (B or A, 188 Hz), with the assignments following from (i) coupling constant magnitude and (ii) a cross-peak between C and P_{ax} in the triple-resonance study. An attempt to establish the assignments of A and B from the possible long-range trans coupling between A and G in a complementary $^{13}C-^{13}C$ correlation spectroscopy (COSY) experiment was unsuccessful. The low relative abundance (3%) of **5c** in solution has frustrated efforts to definitively assign its coordination geometry. The $^{31}P-^{31}P$ coupling (and lack of $^{31}P-^{183}W$ coupling or any examples in which phosphine ligates to tungsten in this system) is only consistent with a trans-disposed $P_{rad}IrIrP_{rad}$ arrangement. Steric arguments then militate against the apical Cp being inclined to the WIr_2 face. Inclination of the apical Cp to either of the W_2Ir faces favors an axially ligated basal Cp. The likely configuration is thus **5c** (Figure 8), for which six signals of equivalent intensity were observed at 193 K, with the remaining two resonances presumably concealed by signals from the more abundant isomers. Resonances were not sufficiently intense to observe ^{183}W-coupled satellites; consequently, the assignment is made with extreme caution. The presence of W−Ir bridging carbonyl signals, axial/apical Ir-ligated carbonyl resonances, and two radially ligated phosphines is only consistent with a WIr_2 basal plane and an apical tungsten atom. The two resonances at high field (167.2, 10 Hz; 163.8, 10 Hz) both display $^{2}J_{CP}$ coupling and are therefore assigned to *f* and *g*. The remaining resonances at 244.9 (*c* or *d*), 228.2 (*e*), 221.3 (*h*), and 215.9 ppm (*a* or *b*) can be assigned by analogy with related clusters discussed above.

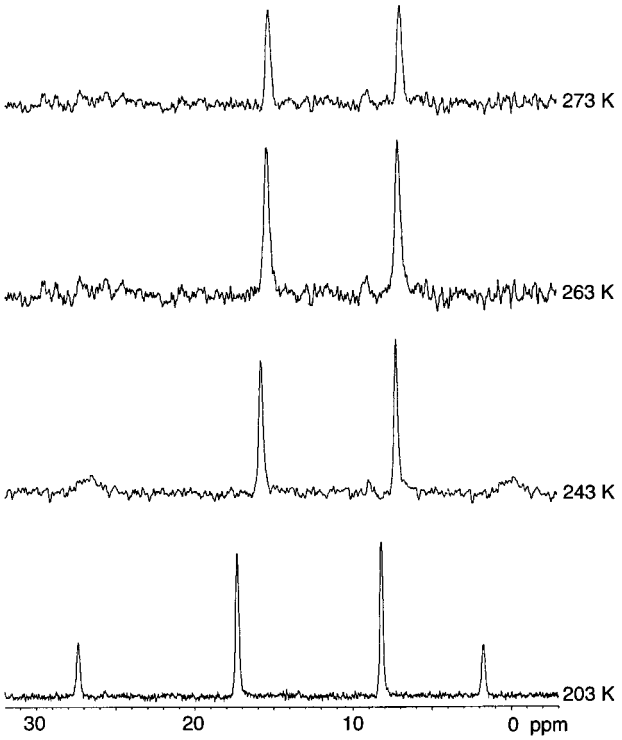

Figure 15. Variable-temperature ^{31}P NMR spectroscopic study of $Cp_2W_2Ir_2(\mu\text{-}CO)_3(CO)_5(PPh_3)_2$ (**3**) in CD_2Cl_2 at 121.4 MHz.

NMR Spectra of $Cp_2W_2Ir_2(\mu\text{-}CO)_3(CO)_5(PPh_3)_2$ (3). The coalescence point in the ^{31}P and ^{13}C NMR spectra of **3** could not be reached due to decomposition of the cluster above 273 K. Due to this poor thermal stability, well-resolved NMR spectra of **3** were difficult to obtain. The ^{31}P and ^{13}C NMR spectra at 203 K (Figures 15 and 16) reveal resonances corresponding to two isomers in the ratio 4:1. Both isomers contain eight resonances of equal intensity in the ^{13}C NMR spectrum at 203 K. Following our arguments above, signals in the W−Ir(μ-CO) region, and only one resonance in the apical/axial Ir−CO region, are consistent with a WIr_2 basal plane and Ir-ligated phosphines in radial and axial sites for both isomers. Resonances are not sufficiently sharp to resolve $^{183}W-^{13}C$ coupling; as with **5c**, assign-

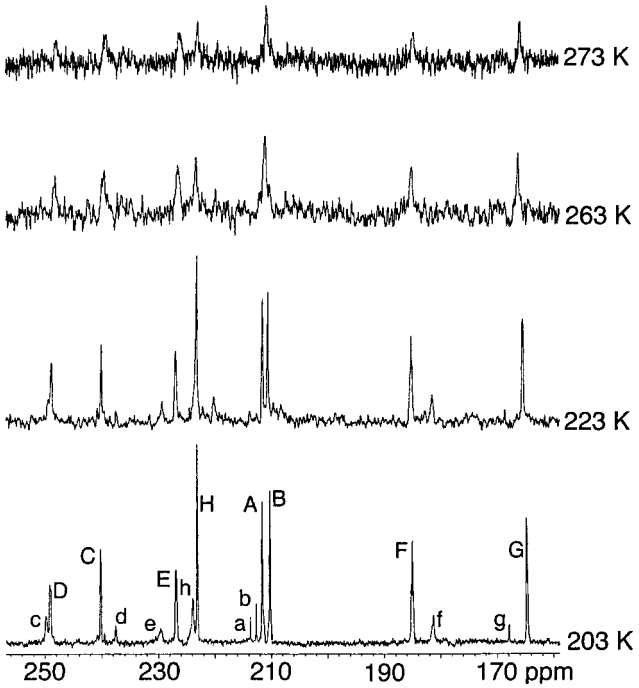

Figure 16. Variable-temperature ^{13}C NMR spectroscopic study of $Cp_2W_2Ir_2(\mu\text{-}CO)_3(CO)_5(PPh_3)_2$ (**3**) in CD_2Cl_2 at 75.4 MHz.

ments are therefore cautious. The major isomer contains resonances at 249.1, 240.1, 226.9, 223.1, 211.5, 210.7, 185.0, and 164.6 ppm, while the minor isomer contains signals at 249.8, 238.0, 229.9, 223.9, 214.0, 212.9, 181.2, and 158.0 ppm. There are six configurations consistent with the phosphine disposition (inclining the apical Cp to any of three accessible faces, and placing the basal Cp axial or radial), one of which is electronically disfavored (the transoid CpWWCp arrangement) and one of which is sterically disfavored (inclining the apical Cp to a $WCp_{ap}WCp_{rad}IrP_{rad}$ face). Of the remaining four possible configurations, two are analogues of **5a** and **5b**, the third involves interchanging Cp_{ax} and h in **5a**, and the fourth involves exchanging Cp_{ap} and b in **5a**. While PPh_3 analogues of **5a** and **5b** minimize steric repulsion, we cannot exclude the other two possibilities at present.

Discussion

The studies above demonstrate the difficulty of definitively assigning carbonyl resonances in transition-metal clusters. Replacement of iridium by tungsten in proceeding from homometallic $Ir_4(CO)_{12}$ to heterometallic $CpWIr_3(CO)_{11}$ and $Cp_2W_2Ir_2(CO)_{10}$ leads to a significantly increased dispersion in chemical shifts of the carbonyl ligands: W−Ir bridging CO (221−257 ppm) > Ir−Ir bridging CO (205−231 ppm) ≈ W terminal CO (206−228 ppm) > Ir radial CO (175−187 ppm) > Ir axial CO (158−166 ppm) ≈ Ir apical CO (159−173 ppm), which facilitates assignment. The presence of the NMR-active 15% abundant ^{183}W isotope permits discrimination of Ir−Ir bridging CO and W terminal CO resonances. Nevertheless, ambiguities remain: the ^{13}C NMR spectra of the clusters reveal no logical way of distinguishing between radial and axial ligated W-bound carbonyls or of determining over which WMIr face (M = W, Ir) apical W-bound carbonyls are inclining. We

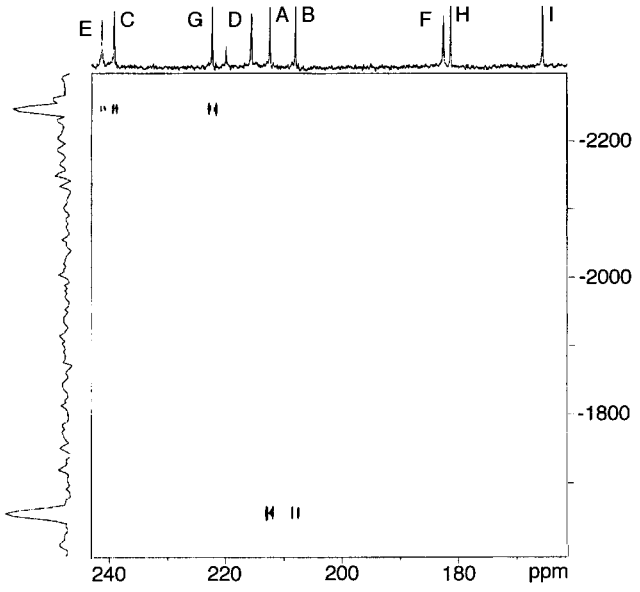

Figure 17. $^{183}W-^{13}C$ correlation NMR spectrum of $Cp_2W_2Ir_2(\mu\text{-}CO)_3(CO)_6(PMe_3)$ (**4**) in CD_2Cl_2 at 203 K at 600.13 (^1H) MHz (after skyline projection).

have therefore resorted to 2D NMR techniques, including triple-resonance experiments, in an attempt to completely assign spectra. The identification of long-range trans coupling between axially ligated W-bound carbonyls and apical carbonyls in $^{13}C-^{13}C$ COSY experiments has been useful in some instances,[7] although poor sensitivity and small coupling constants have rendered this experiment unsatisfactory on many occasions. We have previously used $^{183}W-^{13}C$ and $^{183}W-^{1}H$ correlation experiments to identify the coupling (^1J for $^{183}W-^{13}C$ experiments, ^2J and ^3J for $^{183}W-^1H$ experiments) in $Cp_2W_2Ir_2(\mu\text{-dppm})(CO)_3(CO)_5$,[22] for which a considerable difference in chemical shifts between apical tungsten atoms (−1613 ppm, CD_2Cl_2) and tungsten atoms ligated by cyclopentadienyl groups in axial sites (−2289 ppm) was noted. In the present studies, a similar result was found in the $^{183}W-^{13}C$ correlation spectrum of **4** (tungsten atom ligated by axial cyclopentadienyl group −2247 ppm, apical tungsten atom −1657 ppm), consistent with the assignment of an axial, apical configuration of the η^5-cyclopentadienyl ligands (Figure 17). The lack of ^{183}W NMR data for a definitively assigned radial Cp ligated tungsten atom and the general unpredictability of transition-metal NMR chemical shifts means that at present we cannot comment on the utility of this procedure in distinguishing axial/radial Cp.

$^1H-^{31}P-^{13}C$ triple-resonance NMR spectroscopy and HSQC experiments have proven very useful. A number of ligand-substituted derivatives of $CpWIr_3(CO)_{11}$ and **1** have been structurally characterized with a η^5-cyclopentadienyl ligand and a P-donor ligand located in a transoid arrangement with respect to a W−Ir vector (e.g. $CpWIr_3(\mu\text{-}CO)_3(CO)_7(PMe_3)$,[6] $CpWIr_3(\mu\text{-}CO)_3(CO)_7(PMe_2Ph)$,[13] $CpWIr_3(\mu\text{-dppm})(\mu\text{-}CO)_3(CO)_6$,[23] $CpWIr_3(\mu\text{-dppe})(\mu\text{-}CO)_3(CO)_6$,[23] $Cp_2W_2Ir_2(\mu\text{-}CO)_3(CO)_5\{P(OMe)_3\}_2$,[24] and $Cp_2W_2Ir_2(\mu\text{-dppm})(\mu\text{-}CO)_3(CO)_5$[19]). These instances

(22) Waterman, S. M.; Humphrey, M. G.; Lee, J. *J. Organomet. Chem.*, submitted for publication.

(23) Lee, J.; Humphrey, M. G.; Hockless, D. C. R.; Skelton, B. W.; White, A. H. *Organometallics* **1993**, *12*, 3468.

should be amenable to study by a 2D ($^{31}P-^{13}C$) correlation. However, the proton-detected $^{1}H-^{31}P-^{13}C$ triple-resonance experiment should be more useful due to its increased sensitivity over the ^{31}P-detected technique, particularly when PMe_3 ligands are present. A review containing phosphorus-detected $^{1}H-^{31}P-^{13}C$ triple-resonance experiments has recently been published.[15] In the present study, we have utilized the HSQC experiment to confirm the linear arrangement of axial phosphine and apical η^5-cyclopentadienyl ligands in **4** and **5b**. Coupling from the axially ligated phosphine to the adjacent W−Ir bridging carbonyl detected in the triple-resonance study was utilized in the assignment of carbonyl E in **4** and carbonyls c and C in **5a** and **5b**, respectively.

The configurations assigned to the PMe_3 derivatives seem secure, but the geometry of the mono-PPh_3 isomers is not completely certain, and that of the bis-PPh_3 isomers remains uncertain. A combination of steric and electronic arguments suggests that the major isomer of **3b** adopts the configuration of **5b**, while the minor isomer likely has the ligand disposition of **5a**, but this remains speculative. Experimental difficulties precluded the comprehensive NMR studies which are required, as shown by our work with the PMe_3 derivatives.

The geometries adopted by the crystallographically and spectroscopically well-defined isomers of **2**−**5** can be contrasted with those of related derivatives from the tungsten−triiridium and tetrairidium systems. Trisubstituted derivatives of $Ir_4(CO)_{12}$ usually adopt diradial, axial geometries with monodentate ligands (radial, diaxial ligation is preferred with bidentate ligands), whereas trisubstituted derivatives of $CpWIr_3(CO)_{11}$ (considering Cp as a ligand, i.e., bis(phosphine/phosphite) derivatives) adopt radial, diaxial, or triradial coordination modes.[7,25] Trisubstituted derivatives of $Cp_2W_2Ir_2(CO)_{10}$ (**1**) (i.e. mono(phosphine) derivatives) in the present work adopt diaxial, apical coordination geometries, variants enforced by the fact that a W_2Ir basal plane is unfavorable. Tetrasubstituted derivatives of $Ir_4(CO)_{12}$ adopt radial, diaxial, apical ligation (with the apical ligand oriented toward the axial substituents) to minimize unfavorable steric interactions, the preferred ligand disposition at tris(phosphine) derivatives of $CpWIr_3(CO)_{11}$. Tetrasubstituted derivatives of $Cp_2W_2Ir_2(CO)_{10}$ (**1**) (i.e. bis(phosphine) derivatives) from the current studies favor this geometry but also adopt a configuration corresponding to rotation at the apical tungsten atom, placing the bulky Cp over a radial phosphine containing W_2Ir face. This latter geometry has been shown conclusively only for the sterically less demanding PMe_3 ligand.

Acknowledgment. We thank the Australian Research Council for support of this work and Johnson-Matthey Technology Centre for the generous loan of $IrCl_3$. M.G.H. was an ARC Australian Research Fellow and currently holds an ARC Senior Research Fellowship.

Supporting Information Available: Tables of X-ray crystallographic data for **2a** and figures giving variable-temperature ^{1}H NMR data for **2**, **4**, and **5** and ^{1}H NOESY experimental results for **2**, **4**, and **5**. This material is available free of charge via the Internet at http://pubs.acs.org.

OM9810246

(24) Waterman, S. M.; Humphrey, M. G.; Hockless, D. C. R. *J. Organomet. Chem.*, in press.

(25) Waterman, S. M.; Humphrey, M. G.; Hockless, D. C. R. *J. Organomet. Chem.* **1998**, *555*, 25.